Gondwana Research 22 (2012) 658–663

Contents lists available at SciVerse ScienceDirect

Gondwana Research

journal homepage: www.elsevier.com/locate/gr

GR letter

Dynamic topography and anomalously negative residual depth of the Argentine Basin

G.E. Shephard [a,*], L. Liu [b,1], R.D. Müller [a], M. Gurnis [b]

[a] School of Geosciences, University of Sydney, Sydney, 2006, Australia
[b] Seismological Laboratory, California Institute of Technology, Pasadena, CA, 91125-2100, USA

ARTICLE INFO

Article history:
Received 25 September 2011
Received in revised form 11 December 2011
Accepted 12 December 2011
Available online 27 December 2011

Handling Editor: A. Aitken

Keywords:
Dynamic topography
Residual basement depth
Geodynamic modeling
Argentine Basin
Subduction
Plate tectonics

ABSTRACT

A substantial portion of Earth's topography is known to be caused by the viscous coupling of mantle flow to the lithosphere but the relative contributions of shallow asthenospheric flow versus deeper flow remains controversial. The Argentine Basin, located offshore of the Atlantic margin of southern South America, is one of the most anomalously deep ocean regions as it is significantly deeper than its age would suggest. Previously, the anomalous depth has been attributed to asthenospheric flow and the coupling of the South American plate's westward motion to the shallow mantle. Using a combination of geophysical observations and geodynamic modeling we propose that subducted slab-driven dynamic topography has primarily driven the long-wavelength anomalous residual basin depth since the opening of the South Atlantic. Using an inverse mantle convection model with plate motions since the early Cretaceous, we suggest that the median of present-day dynamic topography of the basin is −400 m. When the residual basement depth is low-pass filtered the depth anomaly is −730 m, suggesting that more than half of the residual basement depth can be attributed to deep-seated mantle dynamics. We conclude that coupled plate tectonic–mantle convection models tied to seismic tomography, bathymetry and sediment thickness data can help to elucidate the driving forces behind Earth's topography, one of the most fundamental characteristics of this planet.

1. Introduction

Since 140 Ma the South American continent has experienced significant changes in relative and absolute plate motions and plate boundary evolution. The opening of the Atlantic Ocean and the westward motion of South America are coupled with the subduction of the oceanic Farallon, Phoenix and Nazca plates along the western margin. Over time, subduction has imparted viscous forces on the overlying continent, leading to the uplift and crustal deformation of the Andes and associated foreland basins (e.g. Isacks, 1988; Kley et al., 1999), as well as anomalous continental subsidence and uplift attributed to dynamic topography (Shephard et al., 2010).

It is well established that mantle convection imparts an influence on surface plate dynamics and the surface expression of such deep-earth processes is manifested in large-scale and non-isostatic vertical motions also termed "dynamic topography". Anomalous continental subsidence and uplift of South America leading to the mid-Miocene disappearance of a large wetland system and formation of the Amazon River has also been recently attributed to dynamic topography (Shephard et al., 2010). Furthermore, global models of present-day dynamic topography (Steinberger, 2007) show that South America exhibits one of the strongest negative dynamic topography signals in the world, with one of the largest negative dynamic signals overlying the Argentine Basin, located offshore of the Atlantic margin of Argentina.

The Argentine Basin represents one of the world's largest oceanic depth anomalies and exhibits a negative residual basement depth of over 1200 m (Crosby et al., 2006). The Argentine Basin also coincides with a long-wavelength free-air global gravity low (Sandwell and Smith, 1997). The amplitude of the Argentine Basin depth anomaly is unusual compared to other regions of oceanic lithosphere of a similar age (Müller et al., 2008a); it is well known through previous studies that old oceanic lithosphere (typically older than ~80 Ma; Parsons and McKenzie, 1978) in some regions of the world exhibit a "flattening" of the age-depth curve that cannot be accounted for by simple thermal subsidence or half-space cooling models (e.g. Phipps-Morgan and Smith, 1992; Hohertz and Carlson, 1998). Consequently, various age-depth curve models for oceanic lithosphere have been constructed to account for these anomalies. These include plate and thermal boundary layer models (e.g. Stein and Stein, 1992; Crosby et al., 2006) as well as asthenospheric flow models, which are a function of shear-induced flow from the absolute plate motion and pressure-induced flow from hotspot-ridge flow interaction (e.g. Phipps-Morgan and Smith, 1992).

It has been suggested that the existence of smaller wavelength, and anomalously shallow, features in the center of the Argentine Basin are associated with local free-air gravity anomalies that can be attributed to "local dynamic" processes (Hohertz and Carlson, 1998). Furthermore, Hohertz and Carlson (1998) suggested that a model combining halfspace-cooling and flow in the asthenosphere accounts for the 98%

* Corresponding author at: Madsen Building, School of Geosciences, University of Sydney, NSW, 2006, Australia. Tel.: +61 2 9351 8093(office), +61 416598162(mobile).
E-mail address: grace.shephard@sydney.edu.au (G.E. Shephard).
[1] Present address: Scripps Institution of Oceanography, University of California, San Diego, La Jolla, CA, 92093, USA.

1342-937X/$ – see front matter
doi:10.1016/j.gr.2011.12.005

of the variance of depth in the southern portion of the Argentine Basin. It should be noted, however, that Hohertz and Carlson (1998) only removed topographic wavelengths less than 100 km. We argue that 100 km as a cutoff-wavelength is too small for the remaining basin-wide anomalous residual depth to be considered "long-wavelength".

Unlike previous studies, Steinberger (2007) suggested that based on a mantle flow model for the present, deep mantle convection might be responsible for large-scale surface elevation anomalies in the region. He found that a downward mantle flow rate of over 2 cm/yr for the 410 km and 660 km boundaries may provide the mantle perturbation required for an expression of negative dynamic topography in the Argentine Basin region. The south of South America is a relatively narrow continental mass, and has therefore been in close proximity to the subduction zone(s) that have existed along its western margin, together with the evolving Argentine Basin. Since at least the Valanginian (~125 Myrs ago) as rifting initiated (Larson and Ladd, 1973) and seafloor spreading in the South Atlantic started (120–130 Myrs ago; Fitzgerald et al., 1990), the subduction of slabs may have provided the mechanism required to drive regional negative dynamic topography, thus initiating eastward-propagating anomalous subsidence across South America.

Unlike the basin's bathymetric, physiographic and ecological dynamics, studies of its formation remain poorly examined. Here we

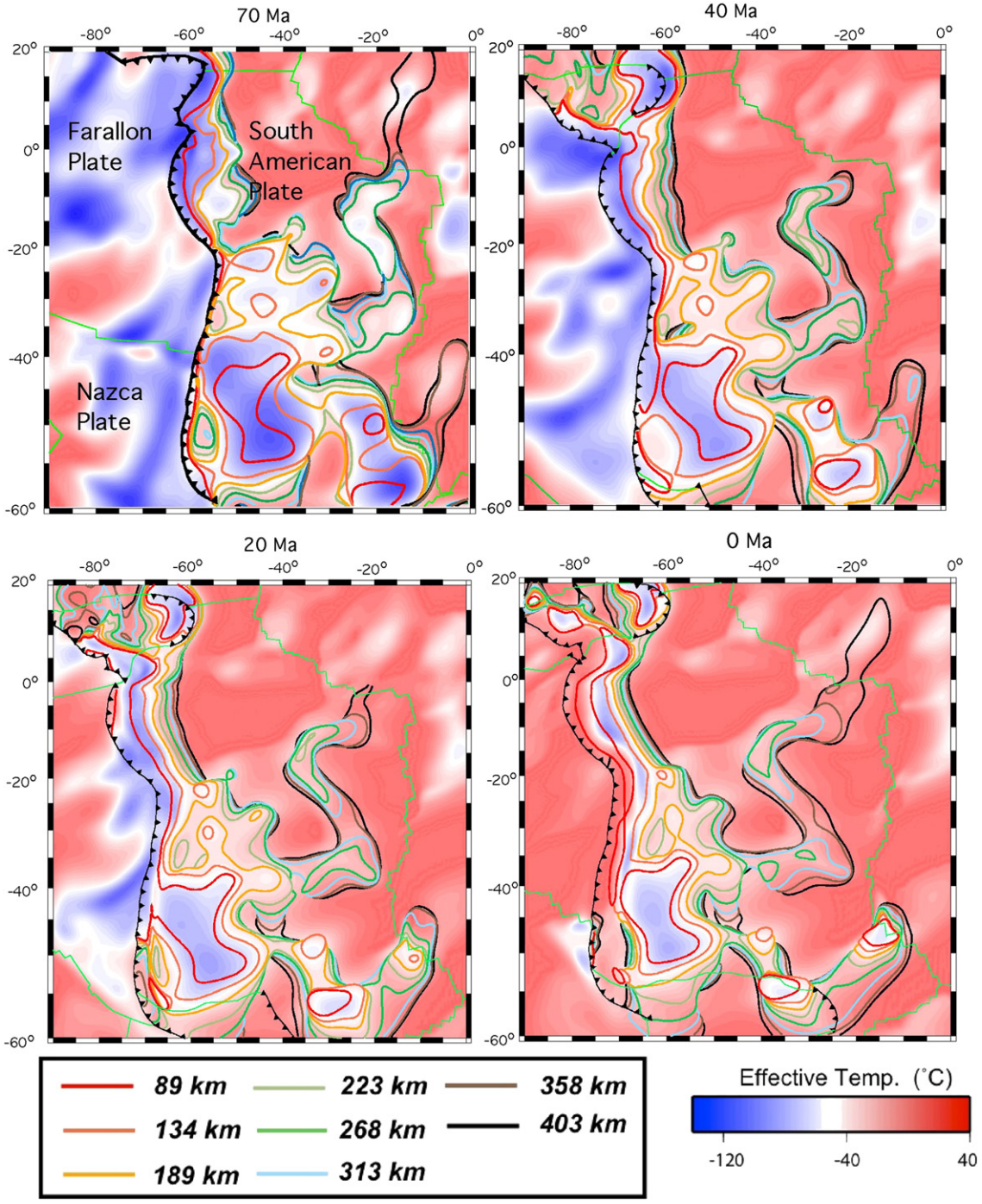

Fig. 1. Horizontal temperature slices at 189 km depth with colored contours showing isotherms of effective-temperature anomalies 40 °C lower than the ambient mantle at different depths. Plate boundaries, including subduction zones and mid-ocean ridges, are also delineated at each reconstructed time step.

propose that the sinking slabs of the subducted Phoenix and Nazca plates (Fig. 1) have imparted a downward viscous pull of the surface lithosphere and contributed, at least in part, to the anomalously negative residual depth of Argentine Basin.

2. Methodology

For robust geodynamic results, the modeling of time-dependent mantle dynamics demands initial conditions and parameters to be well constrained. An iterative procedure that does not rely purely on initial conditions can be achieved using the adjoint method. Initially applied for meteorology and oceanography (Talagrand and Courtier, 1987), adjoint models have been expanded to mantle convection (Bunge et al., 2003; Ismail-Zadeh et al., 2004; Liu and Gurnis, 2008). We ran an inverse model of mantle convection using the iterative adjoint method with the 3-D finite element code *CitcomS 2.1* (http://geodynamics.org; McNamara and Zhong, 2004; Tan et al., 2006). The first approximation of initial conditions for our geodynamic models is optimized through a simple backwards integration of governing equations and refined through an iterative forward-inverse optimization algorithm (Liu and Gurnis, 2008).

Using Grand's (2002) S-wave tomographic inversion, we generate an initial temperature field, scaled at 2×10^3 °C/km/s. We emphasize that this scaling may be different from values obtained by direct laboratory measurements, since ours is an inverse problem where the magnitude of the seismic anomaly is likely smeared during the tomographic inversion. However, this scaling has been successful in other geodynamic models that predict reasonable long-wavelength dynamic topography of North America and northern South America (Spasojevic et al., 2009; Shephard et al., 2010).

We chose to use the S-wave tomography model by Grand (2002) because it is a robust global inversion that captures major mantle structures under southern South America and has been previously employed in successful geodynamic models, particularly when using the adjoint method (Liu et al., 2008; Spasojevic et al., 2009; Shephard et al., 2010). P-wave tomography models may be useful in other regions with good data coverage (unlike the Argentine Basin); however, we previously computed another global geodynamic inverse flow model with the P-wave model of Li et al. (2008) and found that the S-wave model by Grand (2002) is more appropriate in predicting the North American Late-Cretaceous subsidence history with a better spatial match of the flooding maps. The use of shear wave tomography models in constraining depth and resolution has also been shown to best reproduce dynamic topography in other regions (e.g. Boschi et al., 2010). However, it should be noted that the resolution and modeled output of our adjoint model is limited by the resolution of the input tomography. This may account for some longitudinal offset between the modeled dynamic topography and observed residual basement, however we argue that this does not significantly affect our study of long-wavelength features and the correlation to residual basement depth.

Mantle parameters used in these convection models (Table 1) were also utilized in earlier studies (Liu et al., 2008; Spasojevic et al., 2009) in which the depth dependence of mantle viscosity and seismic velocity to density scaling were found by matching Cretaceous stratigraphy of North America. We acknowledge that the magnitude and time-dependence of predicted dynamic topography are influenced by viscosities of both the upper and lower mantle, and the effect of these parameters has been explored in these previous studies. Significantly, these viscosity values for the upper and lower mantle are in the range from data inferred independently from post-glacial rebound (Milne et al., 2004). The mantle is divided into four layers; the lithosphere (0–90 km), upper mantle (90–410 km), transition zone (410–670 km) and lower mantle (670–2891 km) (Fig. 2). The mantle is represented by a temperature-dependent viscosity, and has a non-dimensional viscosity of 100, 0.1, 1 and 15 (relative to 10^{21} Pa s) for the respective mantle layers. The global finite element mesh was composed of 12 caps, with 129×129 nodes in the horizontal and 65 in the radial directions.

To allow for the reconstruction of mantle structure in a context of dynamic and time-dependent plate kinematics, we used the interactive plate-tectonic desktop software package, *GPlates* (https://www.gplates.org; Boyden et al., 2011; Gurnis et al., 2011) to derive surface velocities grids back to 100 Ma. These grids, in 1 Million year increments were imposed as surface boundary conditions on the adjoint model. Our palaeo-plate motions and velocities at each time step were based on the plate model described in Müller et al. (2008a,b). As implemented into the *GPlates* plate reconstructions, the cessation of the Farallon-Phoenix Ridge occurred around 67 Ma, and the Farallon Plate broke into the Nazca and Cocos plates at 23 Ma (Hey, 1977). The geometry of the South American Plate, as delineated by mid-ocean ridges, subduction zones and transform faults, also affects the longitudinal location of subducted slab emplacement and for mantle heterogeneity structure. The model was run from 100 Million years ago to present-day. Subsequent modeling output was manipulated and imaged using *Generic Mapping Tools (GMT)* (Wessel and Smith, 1998).

Dynamic topography, h, is calculated using the consistent boundary flux method (Zhong et al., 2000) by balancing vertical stress and restoring force at the surface:

$$h = \sigma_{rr}/\Delta\rho g \quad (1)$$

where σ_{rr} is the normal of stress in the radial direction, $\Delta\rho$ is the density difference between the mantle and the overlying medium, and g is gravity.

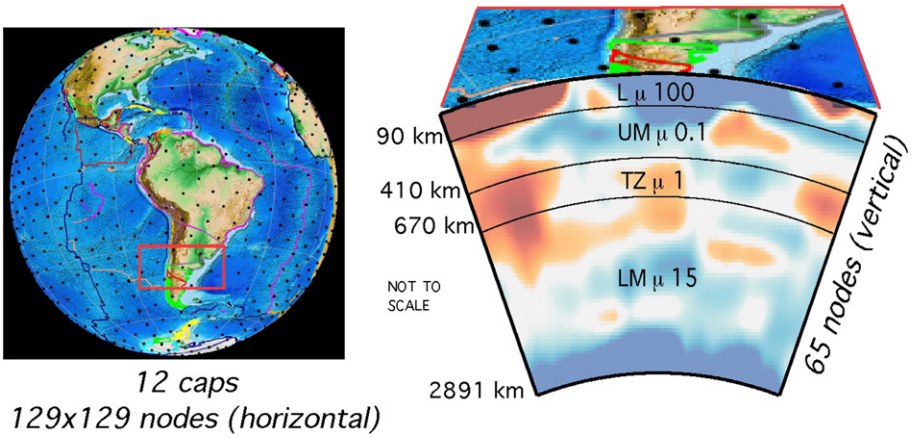

Fig. 2. Simplified model setup with a regional slice showing the four-layer mantle with non-dimensional viscosities superimposed over seismic tomography (Grand, 2002). Nodes of global mesh (black dots, not all shown) were organized into 12 caps each with 129×129 nodes in the horizontal direction and 65 in the radial direction.

Table 1
Mantle parameters used in this study.

Parameter	Value
Reference mantle density	3300 kg/m^3
T at surface	0 °C
Super-adiabatic T change from CMB to surface	400 °C
Radius	6371 km
Coefficient of thermal expansion	3×10^{-5} K^{-1}
Thermal diffusivity	10^{-6} m2/s
Reference viscosity	10^{21} Pa s
Rayleigh number	9×10^{6}

To investigate the effect of dynamic topography on long wavelength topographic features, we generated a global model of averaged residual topography for both continental and oceanic regions. We combined continental topography (ETOPO2), which we corrected for average continental elevation (565 m; Harrison et al., 1983), and a residual basement depth model (Müller et al., 2008a) based on the thermal plate cooling model by Crosby and McKenzie (2009). We subsequently filtered this combined grid, removing wavelengths less than 500 km and passing wavelengths over 750 km (tapered in between). We focus the comparison of dynamic topography and the combined residual depth and elevation grid on the Argentine Basin as delineated in Figs. 3 and 4. Applying a low-pass filter allows for the comparison of long-wavelength signals from dynamic topography to those observed in the anomalous topography/residual basement across the Argentine Basin.

3. Results

Our inverse model of mantle convection shows the evolution of major negative temperature anomalies, mostly interpreted as remnant

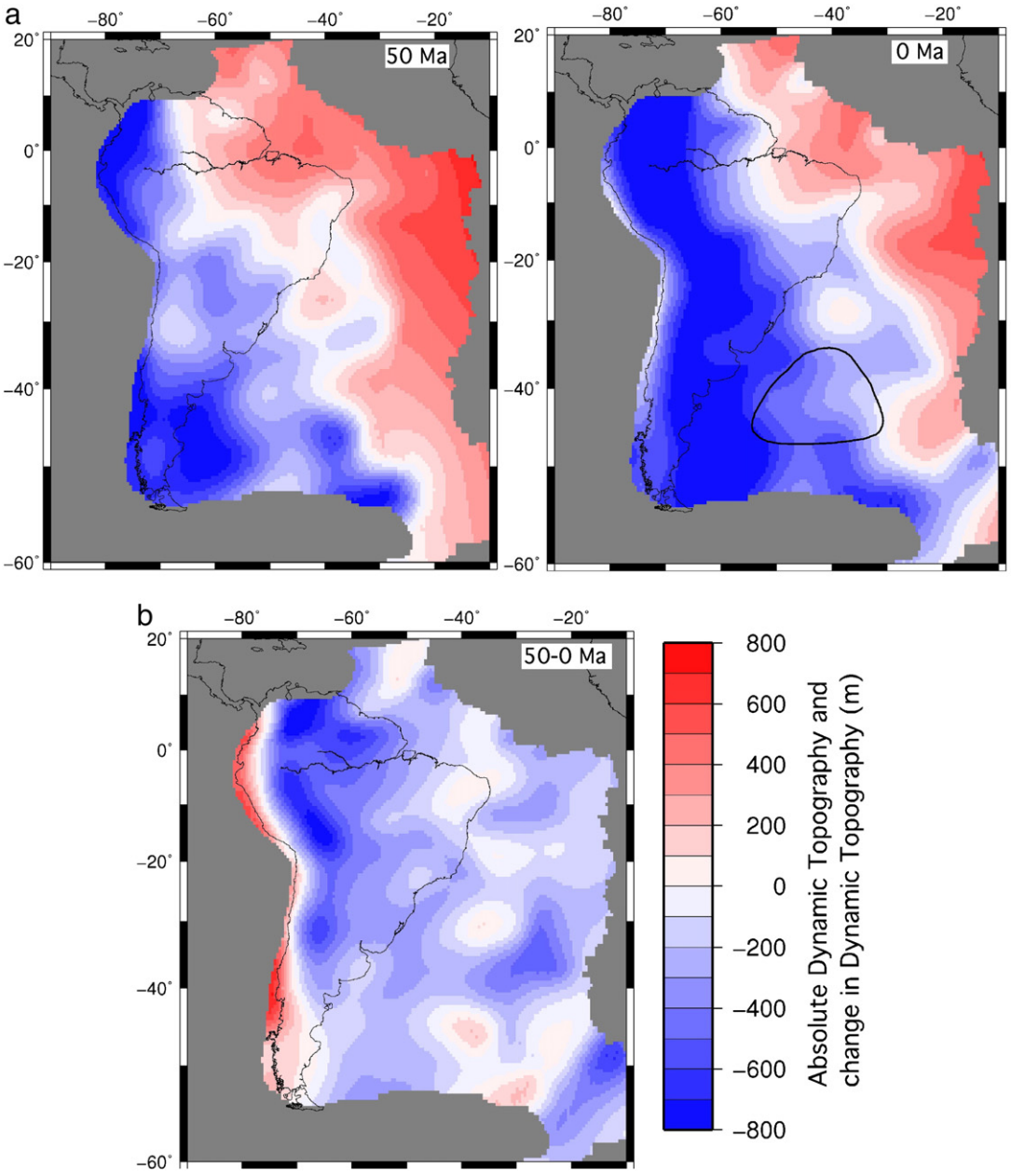

Fig. 3. a) Absolute dynamic topography across South America at 50 Ma and present-day (0 Ma). Blue indicates negative dynamic topography, whereas red indicates positive dynamic topography. Argentine Basin delineated in the subfigure of present-day absolute dynamic topography. b) Change in dynamic topography from 50 Ma-present-day. Blue indicates subsidence whereas red indicates uplift between these times. All maps have been rotated to present-day coordinates, with the present-day coastlines of South America superimposed. Note the fixed color palate between +/−800 m. Gray areas were outside of the model domain.

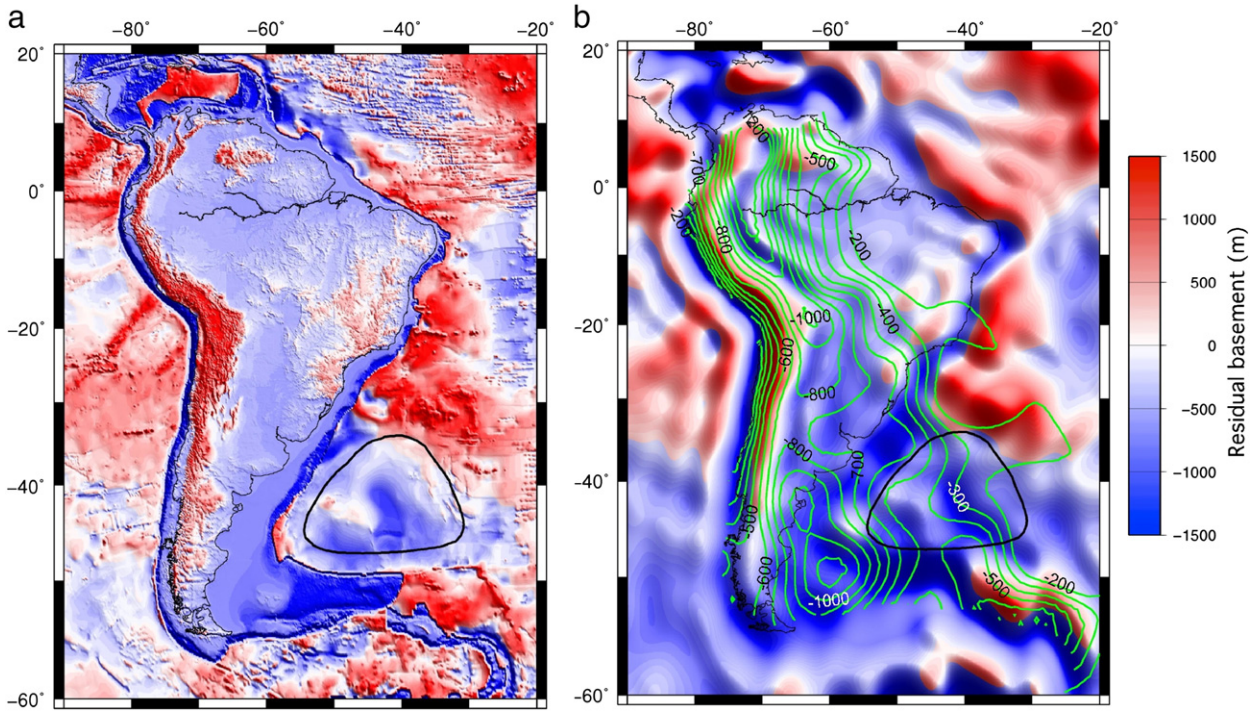

Fig. 4. a) Combined map of continental topography (ETOPO2) corrected for mean continental elevation (563 m; Harrison et al., 1983) and residual basement depth (Crosby and McKenzie, 2009). b) Same as a) but low-pass filtered for wavelengths smaller than 500 km and passed for wavelengths over 750 km. Present-day coastlines and the Argentine Basin are included for reference in black. Contours from present-day dynamic topography (Fig. 2) between −200 m and −1200 m are superimposed in green.

slabs of the Farallon, Phoenix and Nazca plates, under South America (Fig. 1). Throughout time, there is a large amount of lateral slab material under the south of the continent. However, the very shallow sheet-like anomaly (above 200 km) between 35°S and 55°S probably represents a continental lithosphere or an abandoned fossil slab, and a detailed study of this feature is out of the scope of this paper. Slabs under the more northern latitudes (south of 10°N) form a more linear distribution. These subducted slabs represent the movement of the overriding South American Plate over oceanic plates being subducted along its western margin.

Associated with the distribution of cool, sinking, slabs is the surface prediction of long-wavelength and time-dependent deformation, or dynamic topography. From 50 Ma there is an evolving dynamic topographic low of up to −1000 m across South America (Fig. 3). At 50 Ma, the expression of dynamic topography largely consists of two negative signals, in the northwest of the continent and further south, across both continental and oceanic regions. With time, negative dynamic topography shifts eastwards to dominate the continental and southern offshore regions of South America, forming a linear roughly north–south trending signal of up to −1500 m by present-day. Across the Argentine Basin (Fig. 3), present-day dynamic topography expresses a signal in the range of −740 m to 80 m, with a median of −400 m. However, further southwest of the basin, adjacent to the continental shelf margins of southern Argentina, there is a maximum negative dynamic topography signal of over 1100 m. The change in dynamic topography between 50 Ma and present-day predicts broad subsidence across the majority of the continent and offshore Atlantic regions. The viscous sinking of remnants of the Farallon, Phoenix and Nazca plates coupled with the westward motion of the overlying continent has generated a long-wavelength and time-dependent subsidence of ~6 m/Myr on average.

We find that low-pass filtered residual depths in the Argentine Basin (Fig. 4) range from −1670 m to 80 m, with a median of −730 m. The magnitude of anomalous residual basement displays a negative gradient towards the west-southwest of the basin, which also matches the pattern of present-day dynamic topography (Fig. 3). This correlation in magnitude and geometry suggests that to the first order, long-wavelength dynamic topography driven by sinking slab material in the lower mantle is contributing to the anomalous depth of the Argentine Basin. These results are in line with the conclusions of Stein and Stein (1994), suggesting that asthenospheric flow is not exclusively required to match observed and modeled residual oceanic basement depth.

The geodynamic model used here fits a broader range of constraints than traditional shallow asthenosphere models. The model not only accounts for at least half of the large-scale observed residual depth anomaly in the Argentine Basin, but also matches the geological record of time-dependent dynamic topography in North America (Liu et al., 2008; Spasojevic et al., 2009) and northern South America (Shephard et al., 2010) thus providing a robust general mechanism for linking deep mantle structure to surface dynamic topography matching observations from a large region, whereas asthenospheric flow models (e.g. Phipps-Morgan and Smith, 1992) have only been linked to present-day bathymetry.

In delineating the Argentine Basin (Figs. 3 and 4) we have tried to avoid the continental shelf, where regions of high sedimentation and flexural effects may distort the modeled grid of residual topography. While such regions of high sedimentation, lithospheric flexure and dynamic topography were removed in the original models of oceanic basement depth (Crosby and McKenzie, 2009), the inclusion of residual continental topography which has been subsequently low-pass filtered, has added anomalously deep values to our residual basement grid in some continent-ocean boundary locations. This is particularly true in the southern portion of the Argentine Basin, as it is adjacent to the anomalously deep residual basement topography along the Falkland peninsula. It is therefore possible that the long-wavelength residual basement features of the basin are shallower than we suggest. Furthermore, with the magnitude of negative dynamic topography increasing (more negative) towards the southwest, it is also conceivable that dynamic topography contributes to a higher proportion of the anomalously deep residual basement than presented here.

A model comparison by Stein and Stein (1994), focusing on alternative mechanisms for accounting for the observed oceanic basement depth–age relationship in the northwest central North Atlantic and western South Atlantic (i.e. Argentine Basin) showed that an asthenospheric flow model (Phipps-Morgan and Smith, 1992) cannot be reconciled with the combined observed oceanic depths and heat flow in both regions. In particular the northwest central Atlantic constitutes a region where an asthenospheric flow model would presumably be most robust due to the large distance from mid-ocean ridges, hotspots and subduction zones. However, Stein and Stein (1994) found that the asthenospheric flow model vastly over predicts anomalous depth there, leading to the conclusion that there is a fundamental problem with the formulation and application of this model as suggested by Phipps-Morgan and Smith (1992). However, Stein and Stein (1994) did note that return flow models still remain viable and that "regional" deviations may be from asthenospheric flow. This is plausible for the South American Plate, and adjacent regions such as the Argentine Basin, considering the plate has experienced relatively rapid westward motion over the Cenozoic and is currently moving at 2.8 cm/yr (Silver et al., 1998).

We suggest that the residual depth of the Argentine Basin have been driven in the most part by dynamic topography as produced by deep-mantle slab sinking. We also acknowledge that an additional mechanism(s) is required to account for at least another ~400 m of anomalous deepening, and this maybe be explained with asthenospheric flow. The combination of dynamic subsidence from these mechanisms may be comparable to another study (Winterbourne et al., 2009), which suggested that 1 km of anomalous deepening has occurred at the Argentine Basin.

4. Conclusions

The magnitude and location of dynamic topography as predicted from our inverse models of mantle convection provide evidence for deep mantle downwellings as a result of subducted slabs causing, or at least significantly contributing to, the long-wavelength negative residual depth anomaly of the Argentine Basin. Our observation is also supported by the existence of a negative dynamic topography signal in the region of the present-day Argentine Basin since at least 50 Ma, due to long-term subduction in this region, but its expression in oceanic lithosphere is likely to be more recent. Combined with Steinberger's (2007) present-day dynamic topography model and the conclusions of Stein and Stein (1994) regarding anomalous depths of old oceanic lithosphere, our results provide strong evidence that the Argentine Basin anomalous depth is at least partly a result of deeply-seated mantle flow, and not from shallow aesthenospheric flow processes alone (Phipps-Morgan and Smith, 1992; Hohertz and Carlson, 1998). It is also possible that dynamic topography in other regions affected by long-lived subduction may account for regional anomalous flattening of old oceanic lithosphere. While we do not exclude the possibility of asthenospheric flow occurring beneath the Argentine Basin, the correlation in magnitude and location of present-day dynamic to a substantial portion of the regional residual depth anomalies is compelling.

Acknowledgments

Supported by StatOil, NSF Grant EAR-0810303 at Caltech and ARC Grant FL0992245 at Sydney.

References

Boschi, L., Faccenna, C., Becker, T.W., 2010. Mantle structure and dynamic topography in the Mediterranean Basin. Geophysical Research Letters 37. doi:10.1029/2010GL045001.

Boyden, J., Müller, R.D., Gurnis, M., Torsvik, T., Clark, J.A., Turner, M., Ivey-Law, H., Farrow, J., Watson, R., 2011. Next-generation plate-tectonic reconstructions using GPlates. In: Keller, G.R., Baru, C. (Eds.), Geoinformatics: Cyberinfrastructure for the Solid Earth Sciences. Cambridge University Press, Cambridge, pp. 95–114.

Bunge, H.-P., Hagelberg, C.R., Travis, B.J., 2003. Mantle circulation models with variational data assimilation: inferring past mantle flow and structure from plate motion histories and seismic tomography. Geophysical Journal International 152 (2), 280–301.

Crosby, A.G., McKenzie, D., 2009. An analysis of young ocean depth, gravity and global residual topography. Geophysical Journal International 178, 1198–1219.

Crosby, A.G., McKenzie, D., Sclater, J.G., 2006. The relationship between depth, age and gravity in the oceans. Geophysical Journal International 166, 553–573.

Fitzgerald, M.G., Mitchum Jr., R.M., Uliana, M.A., Biddle, K.T., 1990. Evolution of the San Jorge Basin, Argentina. American Association of Petroleum Geologists Bulletin 74, 879–920.

Grand, S.P., 2002. Mantle shear wave tomography and the fate of subducted slabs. Philosophical Transactions of The Royal Society, London A. 360, 2475–2491.

Gurnis, M., Turner, M., Zahirovic, S., DiCaprio, L., Spasojevic, S., Müller, R.D., Boyden, J., Seton, M., Manea, V.C., Bower, D.J., 2011. Plate reconstructions with continuously closing plates. Computers & Geosciences 38, 35–42. doi:10.1016/j.cageo.2011.04.014.

Harrison, C.G.A., Miskell, K.J., Brass, G.W., Saltzman, E.S., Sloan, J.L., 1983. Continental hypsography. Tectonics 2, 357–377.

Hey, R., 1977. Tectonic evolution of the Cocos-Nazca spreading centre. GSA Bulletin 88, 1404–1420.

Hohertz, W.L., Carlson, R.L., 1998. An independent test of thermal subsidence and asthenosphere flow beneath the Argentine Basin. Earth and Planetary Science Letters 161, 73–83.

Isacks, B.L., 1988. Uplift of the central Andean plateau and bending of the Bolivian orocline. Journal of Geophysical Research 93, 3211–3231.

Ismail-Zadeh, A., Schubert, G., Tsepelev, I., Korotkii, A., 2004. Inverse problem of thermal convection: numerical approach and application to mantle plume restoration. Physics of the Earth and Planetary Interiors 145, 99–114.

Kley, J., Monaldi, C.R., Salfity, J.A., 1999. Along-strike segmentation of the Andean foreland; causes and consequences. Tectonophysics 301, 75–94.

Larson, R.L., Ladd, J.W., 1973. Evidence for the opening of the South Atlantic in the Early Cretaceous. Nature 246, 209–212.

Li, C., van der Hilst, R.D., Engdahl, E.R., Burdick, S., 2008. A new global model for P wave speed variations in Earth's mantle. Geochemistry, Geophysics, Geosystems 9. doi:10.1029/2007GC001806.

Liu, L., Gurnis, M., 2008. Simultaneous inversion of mantle properties and initial conditions using an adjoint of mantle convection. Journal of Geophysical Research 113. doi:10.1029/2008JB005594.

Liu, L., Spasojevic, S., Gurnis, M., 2008. Reconstructing Farallon plate subduction beneath North America back to the Late Cretaceous. Science 322, 934–938.

McNamara, A.K., Zhong, S.J., 2004. Thermochemical structures within a spherical mantle: superplumes or piles? Journal of Geophysical Research 109. doi:10.1029/2003JB002847.

Milne, G.A., Mitrovica, J.X., Davis, J.L., Scherneck, H.G., Johansson, J.M., Koivula, H., Vermeer, M., 2004. Continuous GPS measurements of postglacial adjustment in Fennoscandia, 2: modeling results. Journal of Geophysical Research 109. doi:10.1029/2003JB002619.

Müller, R.D., Sdrolias, M., Gaina, C., Roest, W.R., 2008a. Age, spreading rates and spreading asymmetry of the world's ocean crust. Geochemistry, Geophysics, Geosystems 9. doi:10.1029/2007GC001743 Q04006.

Müller, R.D., Sdrolias, M., Gaina, C., Steinberger, B., Heine, C., 2008b. Long-term sea-level fluctuations driven by ocean basin dynamics. Science 319, 1357–1362.

Parsons, B., McKenzie, D., 1978. Mantle convection and the thermal structure of the plates. Journal of Geophysical Research 83, 4485–4496.

Phipps-Morgan, J.P., Smith, W.H.F., 1992. Flattening of the sea-floor depth-age curve as a response to asthenospheric flow. Nature 359, 524–527.

Sandwell, D.T., Smith, W.H.F., 1997. Marine gravity anomaly from Geosat and ERS 1 satellite altimetry. Journal of Geophysical Research 102, 10039–10054.

Shephard, G.E., Müller, R.D., Liu, L., Gurnis, M., 2010. Miocene drainage reversal of the Amazon River driven by plate-mantle interaction. Nature Geoscience 3, 870–875.

Silver, P.G., Russo, R.M., Lithgow-Bertelloni, C., 1998. Coupling of South American and African plate motion and plate deformation. Science 279, 60–63.

Spasojevic, S., Liu, L., Gurnis, M., 2009. Adjoint models of mantle convection with seismic, plate motion and stratigraphic constraints: North America since the Late Cretaceous. Geochemistry, Geophysics, Geosystems 10. doi:10.1029/2008GC002345.

Stein, C.A., Stein, S., 1992. A model for the global variation in oceanic depth and heat-flow with lithospheric age. Nature 359, 123–129.

Stein, C.A., Stein, S., 1994. Comparison of plate and asthenospheric flow models for the thermal evolution of oceanic lithosphere. Geophysical Research Letters 21, 709–712.

Steinberger, B., 2007. Effects of latent heat release at phase boundaries on flow in the Earth's mantle, phase boundary topography and dynamic topography at the Earth's surface. Physics of the Earth and Planetary Interiors 164, 2–20.

Talagrand, O., Courtier, P., 1987. Variational assimilation of meterological observations with the adjoint vorticity equation. 1: theory. Quarterly Journal of the Royal Meterological Society 113, 1311–1328.

Tan, E., Choi, E., Thoutireddy, P., Gurnis, M., Aivazis, M., 2006. GeoFramework: coupling multiple models of mantle convection within a computational framework. Geochemistry, Geophysics, Geosystems 7. doi:10.1029/2005GC001155.

Wessel, P., Smith, W.H.F., 1998. New, improved version of the Generic Mapping Tools released. EOS Transactions AGU 79, 579.

Winterbourne, J., Crosby, A., White, N., 2009. Depth, age and dynamic topography of oceanic lithosphere beneath heavily sedimented Atlantic margins. Earth and Planetary Science Letters 287, 137–151. doi:10.1016/j.epsl.2009.08.019.

Zhong, S., Zuber, M.T., Moresi, L., Gurnis, M., 2000. The role of temperature-dependent viscosity and surface plates in spherical shell models of mantle convection. Journal of Geophysical Research 105, 11063–11082.